

DNA Oligomers Containing Alloxazine in Place of Thymine: Interactions Between DNA Strands

Jordan Noel Downing
Biochemistry Departmental Honors Thesis

University of Colorado Boulder
Defense Date: November 1, 2024

Defense Committee:

Dr. Robert Kuchta, Department of Biochemistry - Thesis Advisor
Dr. Joseph Falke, Department of Biochemistry
Dr. Jingshi Shen, Department of Molecular, Cellular, and Developmental Biology

Table of Contents

Abstract	1
Introduction	
Watson-Crick base pairing	2
Alloxazine in DNA	3
Dithionite as a reducing agent	5
Spectroscopy	7
Results	
Generating annealed DNA	9
Visualizing DNA containing alloxazine	11
Dithionite reduces DNA samples	15
Visualizing DNA containing residue P	18
Discussion	20
DNA samples containing alloxazine	21
DNA samples reduced by dithionite	23
Residue P in DNA samples	24
Future directions	25
Materials and Methods	
Annealing DNA samples	27
Preparing reduced samples	28
Visualizing T _m values using spectroscopy	30
Determining concentration of stocks	31
Analysis of T _m values	32
Supplemental Information	33
Acknowledgements	34
References	35
Figures	
(1) The four DNA bases	2

(2) Structures of alloxazine and riboflavin	3
(3) Alloxazine base pairing with adenine	4
(4) The Marschalk reaction	5
(5) Linearly versus circularly polarized light	8
(6) DNA1-A/X strands	10
(7) AK06/X DNA strands	12
(8) Two-alloxazine residue DNA strands	14
(9) DNA samples containing dithionite	16
(10) DNA samples containing 4 uL dithionite	17
(11) DNA samples containing P residues	19
(12) Average T_m and hysteresis effect comparisons	25
(Sup. Figure 1) AKF06/X samples	33
(Eq. 1) The Beer-Lambert Law	31
(Table 1) Canonically base-paired DNA samples	10
(Table 2) DNA1-A and AK06 T_m comparisons	13
(Table 3) T_m values for primer and template strands	33
(Sup. Table 1) DNA sequences containing alloxazine	34

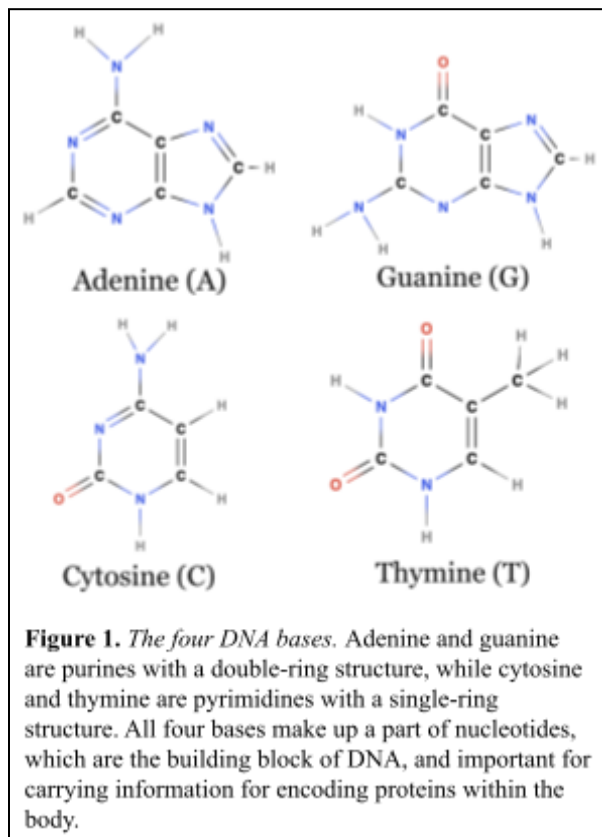
Abstract

Single DNA strands combine to form a double helix structure following Watson-Crick base pairing rules, adenine (A) pairs with thymine (T) and cytosine (C) pairs with guanine (G). However, by introducing a non-standard base called alloxazine into a DNA sequence, the residue can form both normal Watson-Crick base pairs to adenine, or new connections to another non-canonical residue. The number of bonds alloxazine forms depends on the oxidized/reduced state of the residue. A small amount of literature has focused on the base pairing properties of alloxazine. Our research, however, focused on the reduced form of alloxazine paired with a non-standard residue P (2-amino-imidazo[1,2-a]-1,3,5-triazin-4(8H)one). Very little research has been done on residue P, and, to our knowledge, no research has studied DNA samples containing both alloxazine and residue P. It has been previously established that DNA strands containing one or two alloxazine residues takes on the B-form like canonical (standard) DNA. Our research, however, aimed to seek whether the form of DNA changed when alloxazine base paired with residue P. Using dithionite, both the alloxazine in the DNA strands as well as the oxygen in solution were reduced, as reduced alloxazine preferentially forms hydrogen bonds with residue P. Using spectroscopy, we compared the T_m (melting temperature) values of DNA containing standard base pairs, alloxazine, residue P, and/or dithionite. This research provides important information in the fields of biotechnology and robotics. By controlling the interactions between DNA bases, the ability of molecular nanorobots to accomplish specific goals in molecular interactions and personalized medicine is far more achievable.

Introduction

Watson-Crick base pairing

Watson-Crick base pairing refers to the bonds two single DNA strands make with each other to form a right-handed double-stranded double helix shape. The four bases found in DNA are adenine (A), cytosine (C), guanine (G), and thymine (T). Adenine and guanine are purines made up of five carbons and four nitrogens in a two-ring structure. Cytosine and thymine are pyrimidines made up of four carbons and two nitrogens in a single ring structure. For both purines and pyrimidines, the identity of the base is determined by the molecular groups branching off of the main ring structure(s), as shown in Figure 1. The four DNA bases bond with a sugar and phosphate group to form nucleotides. The double helix shape of double-stranded DNA is formed by nucleotide bonding between DNA single strands. Hydrogen bonds form



between the bases within the middle of the helix, and phosphodiester bonds form between the sugar and phosphate groups of two nucleotides in the helix backbone¹.

James Watson and Francis Crick are often credited with the discovery of the double helix structure of DNA in 1953². In the structure of DNA, adenine binds with thymine and guanine binds with cytosine, a breakthrough that would not have happened without the research of many other notable scientists, including Rosalind Franklin³. Adenine and thymine form two

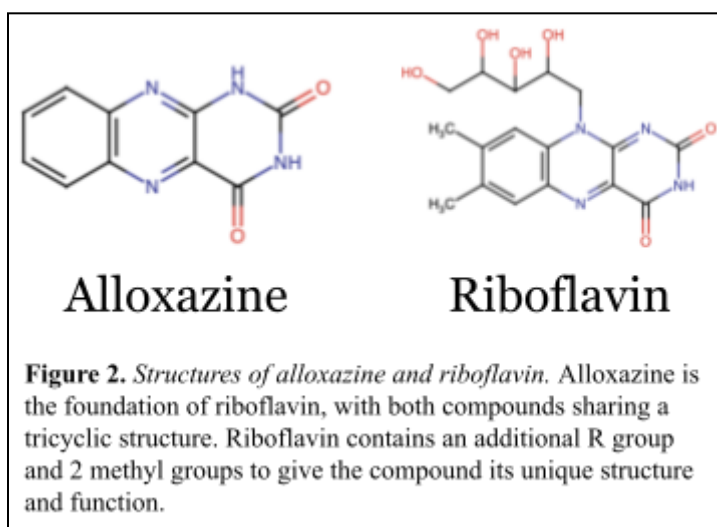
hydrogen bonds between the residues, and cytosine and guanine form three hydrogen bonds. The

hydrogen bonds are caused by the strong electronegativity difference between a hydrogen atom attached to a very electronegative atom, such as N or O, and a strong electronegative atom on the other base. The difference in electronegativity reflects an unequal sharing of electrons between the two atoms, which forms strong non-covalent bonds between the two single strands of DNA.

The hydrogen bonds cause the double-stranded DNA to form a double helix, but the geometry and dimensions of the double helix can vary. The most common form of DNA is B-DNA, which is the type of DNA found in most living organisms. A-DNA is shorter and wider, while Z-DNA is a left-handed double helix⁴. The conditions with which A-DNA and Z-DNA exist vary from those that allow B-DNA to be dominant, and the importance of DNA geometry variations is an ongoing question that this research aims to help answer.

Alloxazine in DNA

Alloxazine (IUPAC name: *1H*-benzo[*g*]pteridine-2,4-dione) is a tricyclic compound that is the foundation of flavins, including riboflavin (vitamin B2). Riboflavin contains a ribitol R group, as well as two methyl groups at positions 2 and 4,⁵ as shown in Figure 2. Riboflavin is a precursor for flavin mononucleotide (FMN) and flavin adenine dinucleotide (FAD)⁶. Both molecules are cofactors for multiple reduction-oxidation enzymes in reactions essential to metabolism.

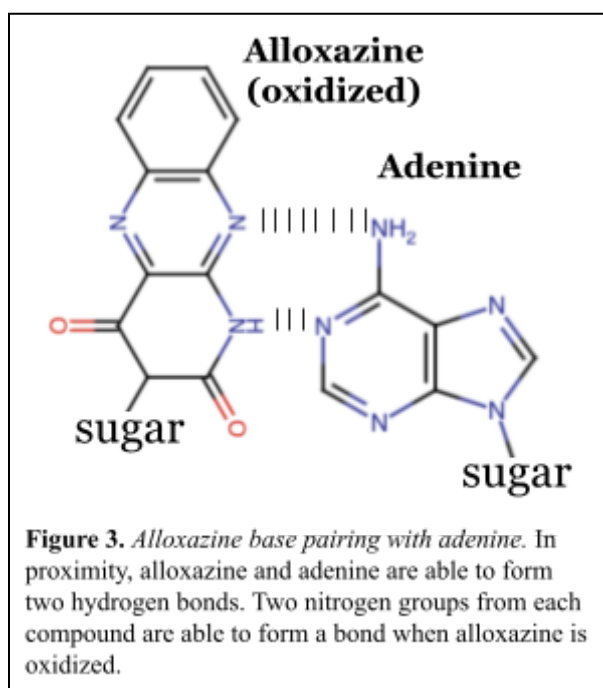


Riboflavin itself can also exist in an oxidized or reduced form, a helpful certainty used during this research to determine if a DNA sample was reduced or oxidized. When riboflavin is

reduced, the compound appears colorless. Riboflavin, however, appears a bright yellow-orange color that can be observed with the naked eye when oxidized.

Unlike riboflavin, the oxidation state of alloxazine is observed through its spectra. Alloxazine has a tautomer, isoalloxazine, that differs in the placement of a hydrogen atom in the molecule. Despite the two compounds having the same formula, they exhibit differences in spectroscopic properties. The isoalloxazine electronic structure is less stable than the alloxazine electronic structure, which causes a hyperchromic shift to significantly shorter wavelengths for each peak in the alloxazine absorbance graph⁷.

Alloxazine can also exist in an oxidized or reduced form. The reduced form of alloxazine



contains amine groups on the central ring, while the oxidized form contains nitrogens bound to the surrounding carbons by double bonds, as shown in Figure 2. The oxidized form of alloxazine binds with Watson-Crick base pairing to adenine residues on the opposite DNA strand, which has one donor and one acceptor group, as shown in Figure 3. When alloxazine is reduced, however, the compound forms a bond with a residue abbreviated as P

(2-amino-imidazo[1,2-a]-1,3,5-triazin-4(8H)one) that has one donor and two acceptor groups⁸.

Because the number of bonds between alloxazine and its base pair varies depending on the state of the alloxazine, the interactions between single DNA strands cause a double helix with slight variations to form. In this research, we looked at how the variations in DNA geometry changed

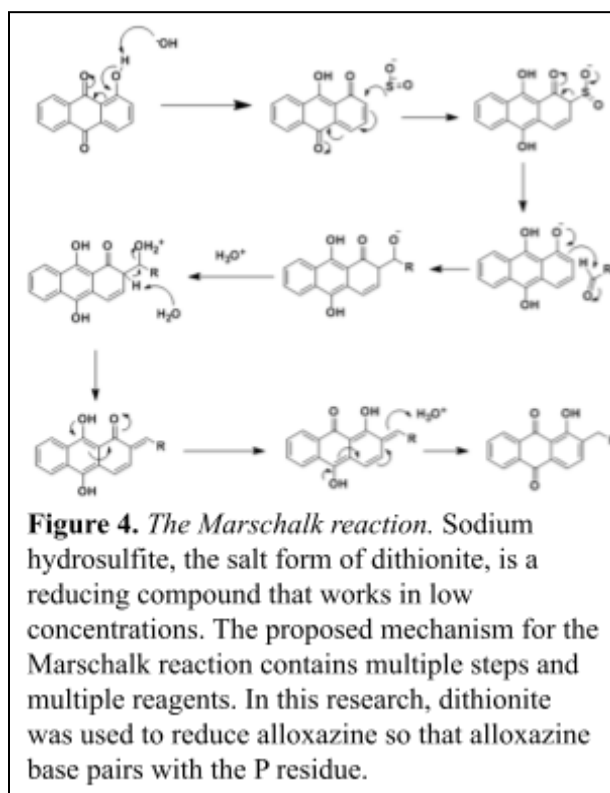
the T_m (melting temperature) of the DNA, which measures the temperature at which DNA is half single-stranded and half double-stranded, providing valuable information on the strength of bonds between nucleotides.

Dithionite as a reducing agent

Throughout this research, dithionite was used to reduce both the alloxazine in DNA and the oxygen in solution. Dithionite is an oxyanion that is usually present as the salt sodium hydrosulfite. The compound is effective at reducing samples in low concentrations and in a short period of time⁹. The Marschalk reaction describes how dithionite reduces phenolic anthraquinones and can be used in the production of substituted phenolic anthraquinones, as shown in Figure 4¹⁰. The research in this paper focused on using the Marschalk reaction to reduce the oxidized form of alloxazine.

Dithionite decomposes quickly in the presence of water into sodium bisulfite (NaHSO_3) and sodium thiosulfate ($\text{Na}_2\text{S}_2\text{O}_3$). The decomposition process is accelerated by high concentration, temperature, and acidity¹¹. Dithionite exposed to oxygen in solution decomposes in a second order reaction at a fast rate due to the increasing concentration of hydrogen sulfite (HSO_3^-) and hydrogen sulfate (HSO_4^-) that make the solution more acidic. To begin the reaction, 1M HEPES

(2-[4-(2-hydroxyethyl)piperazin-1-yl]ethanesulfonic acid) pulls the hydrogen off of the nitrogen



in the first step. HEPES has zwitterion properties and is an effective buffer agent around pH 7¹². Because the reaction takes place in water, the reaction is able to continue propagating until the entirety of the alloxazine is reduced and minimal oxygen exists in solution. Sodium salts serve to stabilize dithionite once reacted with water. In our research, we found that as little as 3 μ L of 0.1M dithionite in 2mL of solution is effective in reducing DNA samples, and that dithionite decomposes to an undetectable level within a day and a half.

The absorbance spectrum of samples containing dithionite make it possible to see if a sample is reduced. UV-Visible spectroscopy shows that reduced samples have a distinct peak around 315 nm that is attributable to dithionite¹³. A distinct peak at 315 nm helps to determine if the sample is continuing to react with the dithionite, and whether the sample contains excess dithionite. The peak at 315 nm disappears when the sample is reoxidized or if the solution of dithionite is exposed to excess oxygen before being added to the sample. The absorbance of dithionite, however, makes the compound a difficult reducing agent in studying DNA. Our research focused on the absorbance of DNA in oxidizing and reducing environments for light at 260 nm. Because dithionite has high absorbance of light at the 260 nm wavelength, and a strong absorbance peak at a longer wavelength (315 nm), the absorbance peaks of dithionite interfered with the DNA spectra.

Dithionite, additionally, has been shown to interfere with the shape of DNA as the molecule is reduced¹⁴. Our research has found that the addition of dithionite to DNA samples results in variations of the typical sigmoidal curve of canonical DNA, as well as lowering the T_m values correlated with the DNA samples.

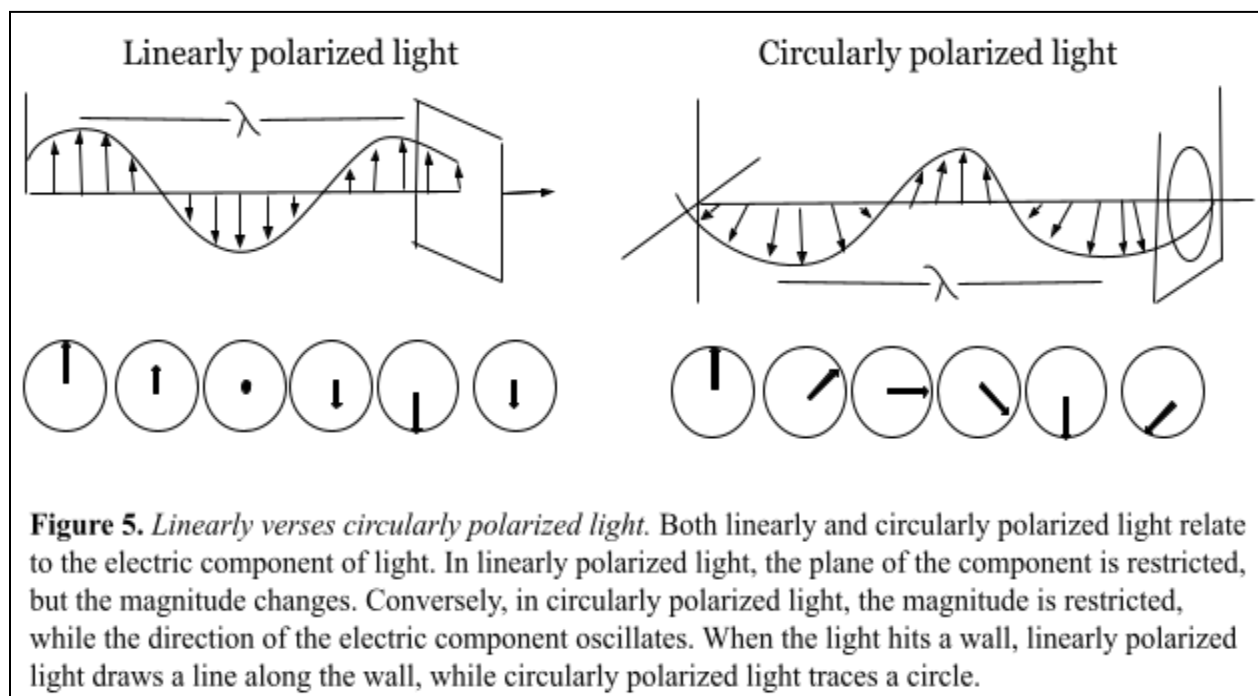
Spectroscopy

Spectroscopy takes advantage of the fact that different materials interact with different wavelengths of light in unique ways. There are multiple kinds of spectroscopy that analyze objects in different areas of the electromagnetic spectrum, including infrared spectroscopy, nuclear magnetic resonance (NMR) spectroscopy, and ultraviolet-visible (UV-Vis) spectroscopy. In this research, we primarily used UV-Vis spectroscopy to analyze the melting temperature of DNA in the absence and presence of a reducing agent. The UV-Vis spectrometer provides the temperature at which half of the DNA in a sample is single-stranded and half is double-stranded during a heat up and cool down cycle, and presents the data as a graph of temperature versus absorbance.

UV-Vis spectrometers measure the amount of discrete wavelengths of ultraviolet or visible light that are absorbed through a sample¹⁵. The visible light region of the electromagnetic spectrum is the region that humans are able to see with their naked eyes, and extends roughly from 750 nm to 400 nm. Ultraviolet waves have higher energy and a shorter wavelength than visible light waves, and the ultraviolet region extends roughly from 400 nm to 100 nm¹⁶.

Single-stranded and double-stranded DNA absorb light differently at 260 nm. The occurrence of single-stranded DNA absorbing more light than double-stranded DNA is called the hyperchromic shift¹⁷. The bases within DNA strongly absorb light, and the base-pair stacking that occurs in double-stranded DNA largely inhibits their absorption of light.

In our research, we also used another spectroscopy technique called circular dichroism (CD) spectroscopy. Circular dichroism uses circularly polarized light to study optically active chiral materials¹⁸. Light is left and right circularly polarized, and the two directions can be isolated to study which kind of light a material prefers to absorb. Light is an electromagnetic wave. The two wave components are caused by the electric field and the magnetic field which



propagate at the speed of light perpendicular to each other. Linearly polarized light is the result of the electric component of the wave being restricted to one plane perpendicular to propagation while the magnitude of the component oscillates. Circularly polarized light, however, results from the electric component having a constant magnitude, but an oscillating direction (Figure 5)¹⁹.

Similarly to UV-Vis spectroscopy, single-stranded DNA and double-stranded DNA absorb circularly polarized light differently due to the helical structure of DNA. The helical twist in double-stranded DNA forms a chiral compound. Because chiral compounds preferentially absorb one direction of circularly polarized light over the other, a circular dichroism measurement for DNA can be made. The difference in structure between single-stranded DNA and double-stranded DNA is caused by a difference in base-pair arrangement, which leads to a difference in light absorption preference, and therefore a difference in circular dichroism measurement²⁰.

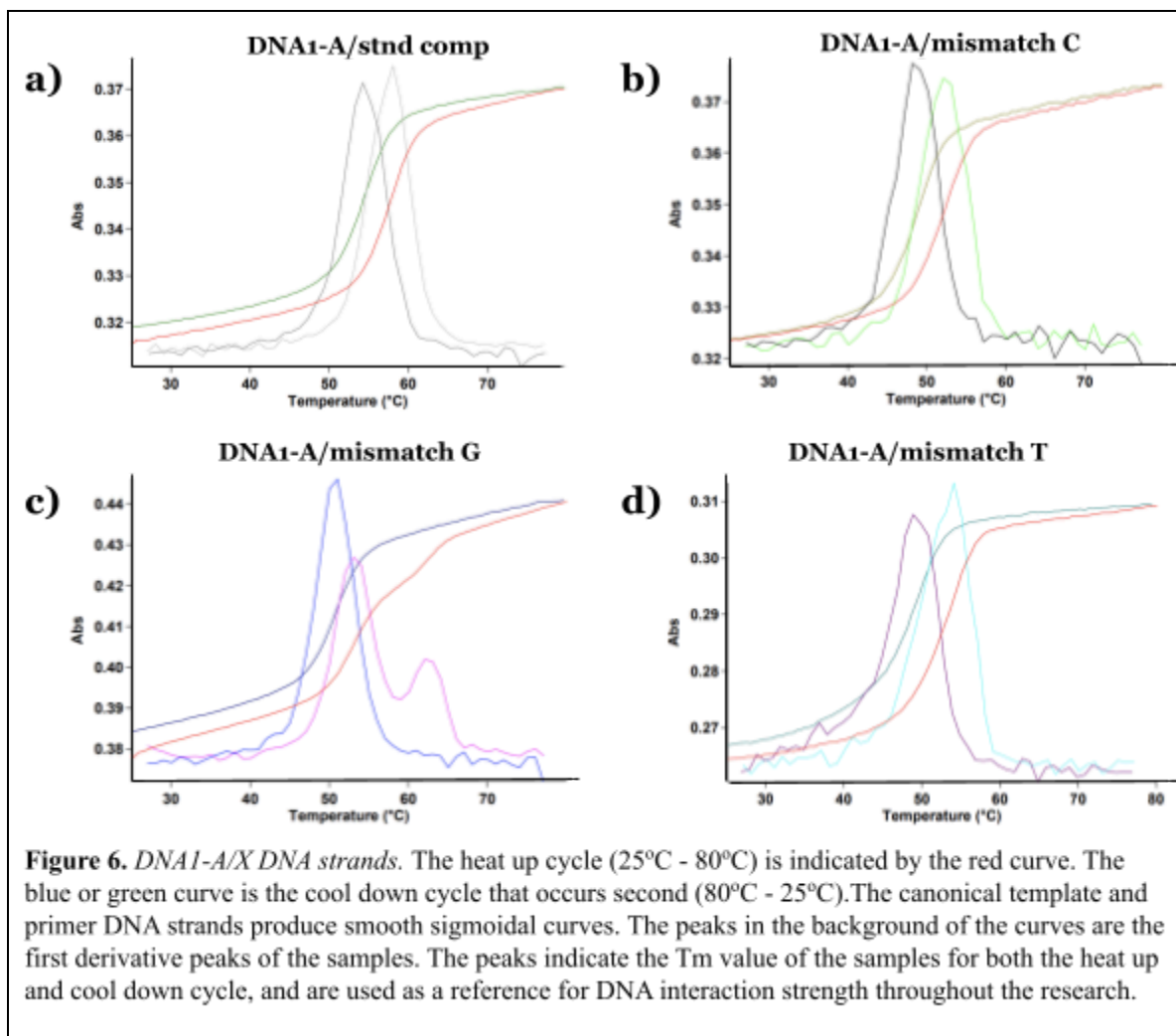
Both UV-Vis and CD spectroscopy are helpful techniques that were used in this research to determine the structure of the DNA within our samples. Electrons in the sample absorb energy and release the energy once they leave the excited state, which sends information about the structure of a material. Both types of spectroscopy produce light in the ultraviolet and visible regions of the electromagnetic spectrum, but the way the light is isolated to interact with the material in the sample varies, illuminating different but vital information about the bond strength and structure of the DNA we studied.

Results

Generating annealed DNA

To design a standard for which to compare non-canonical base pairing DNA, we began by annealing complementary strands of DNA from Integrated DNA Technologies. The 24 base-pair sequences were annealed and run through the UV-Visible spectrometer. The spectrometer produced the temperature versus absorbance curve for the double-stranded DNA as the strands were separated and re-annealed, as shown in Figure 6(a-d). In Figure 6, one template strand, DNA1-A, was run with four separate primer strands labeled as “standard complement”, “mismatch C”, “mismatch G”, and “mismatch T.”

All four graphs produced the expected sigmoidal curve. The curve for the DNA1-A template strand paired with the standard complement generated the smoothest curve, which is expected since the two DNA strands are exact complements. The first derivative graphs also look relatively smooth on all four graphs, with the peak of the graphs indicating the T_m values of each sample. With the exception of DNA1-A paired with mismatch G (Figure 6c) which has two peaks in the first derivative heat up curve, the T_m values can be easily determined visually.



Strand Name	Sequence	Avg T_m Value (w/ DNA1-A)
DNA1-A	TTC CTC TTC TCC TTC TTC TCC TTT	N/A
Standard Complement	AAA GGA GAA GAA GGA GAA GAG GAA	56.2°C
Mismatch C	AAA GGA GAA GAC GGA GAA GAG GAA	50.2°C
Mismatch G	AAA GGA GAA GAG GGA GAA GAG GAA	52.1°C
Mismatch T	AAA GGA GAA GAT GGA GAA GAG GAA	51.5°C

Table 1. *Canonically base-paired DNA samples*

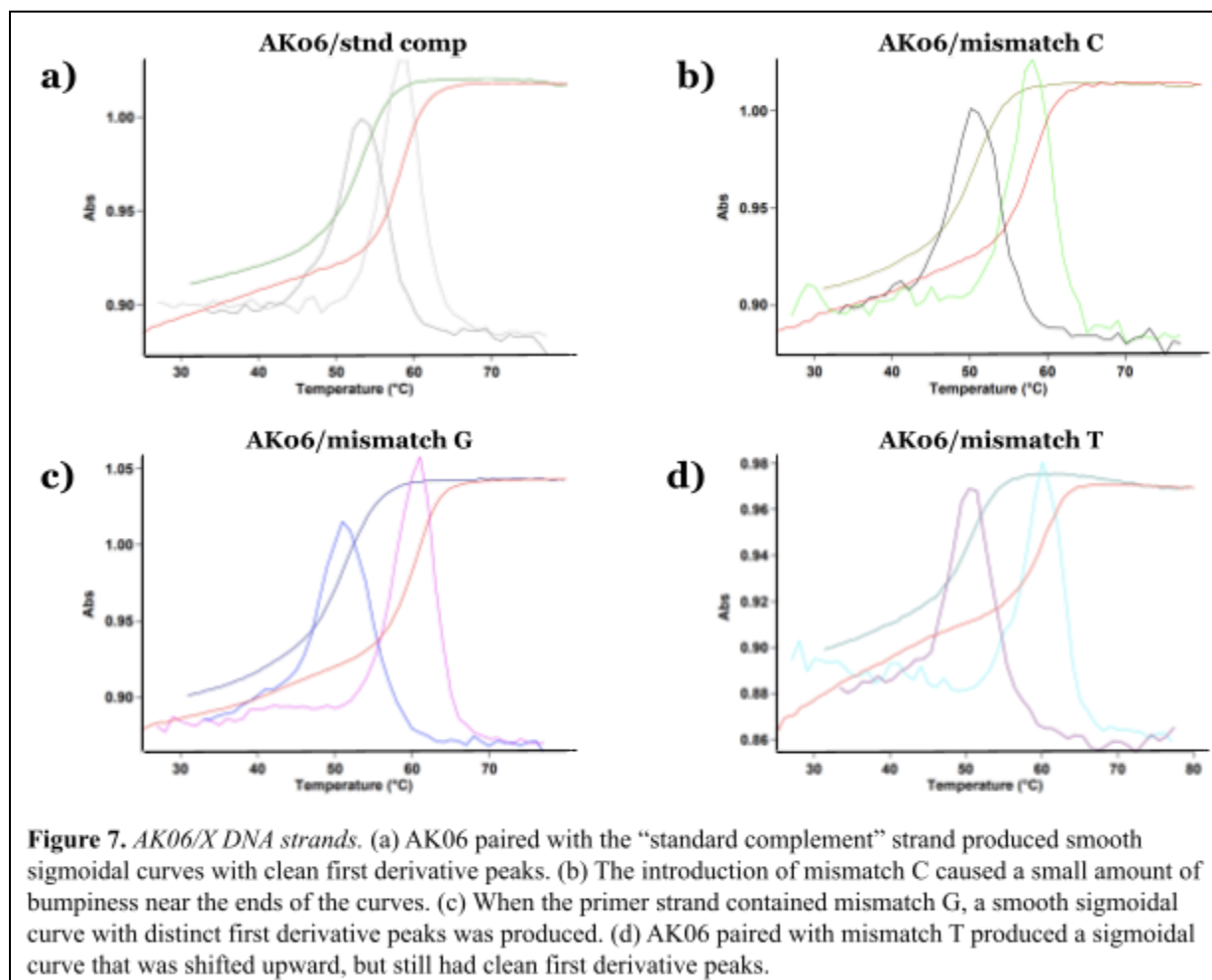
Also as expected, the T_m value for DNA1-A/standard complement is higher than the T_m values for each of the other pairings, as seen in Table 1. The exact complementary base pairing of DNA1-A and the standard complement form stronger and more abundant hydrogen bonds compared to the other three pairings, and therefore requires more energy for the two strands to be separated.

Each strand was tested in at least seven identical experiments and yielded similar results each time. The T_m values and curves proved to be replicable, and the strands were determined to be appropriate for moving forward with experiments.

Visualizing DNA containing alloxazine

After establishing the typical curves and T_m values for canonically base-paired DNA, we began testing each of the four primer strands with a template strand containing either one or two alloxazine residues. A full list of the names and sequences of each alloxazine-containing DNA strand can be found in Supplementary Table 1, but we primarily tested six alloxazine strands. AK06, AKF06, AKF17, and AKF18 each contain one alloxazine residue at a different position in the 24-base sequence. AK014 and AKF14 each contain two alloxazine residues. The DNA template strands containing one alloxazine residue were paired with all four primer strands while the template strands containing two alloxazine residues were paired only with the “standard complement” primer strand. The oxidized alloxazine residues formed bonds with adenine residues on the opposite strand, forming double-stranded DNA, though with slight variations compared to the canonical DNA double helix. The temperature versus absorbance curves for AK06 paired with each primer strand is shown in Figure 7.

The curves for AK06 paired with close-complement primer strands produced sigmoidal curves as expected. When compared to a standard DNA double-helix, however, the gap between



the heat up and cool down curve is quite a bit larger for AK06 strands. The large gap indicates that different interactions occur between the bases and the solvent during heating and cooling of the strands. The high heating T_m values for all four samples in Figure 7 indicates that there are strong interactions between bases on the opposite DNA strands. Once the bases are separated, however, their interactions with the solvent are stronger compared to the base-solvent interactions formed by canonical DNA, as seen by the lower cooling T_m value. This phenomenon is known as the hysteresis effect²¹ and can be seen in multiple examples of phase changes.

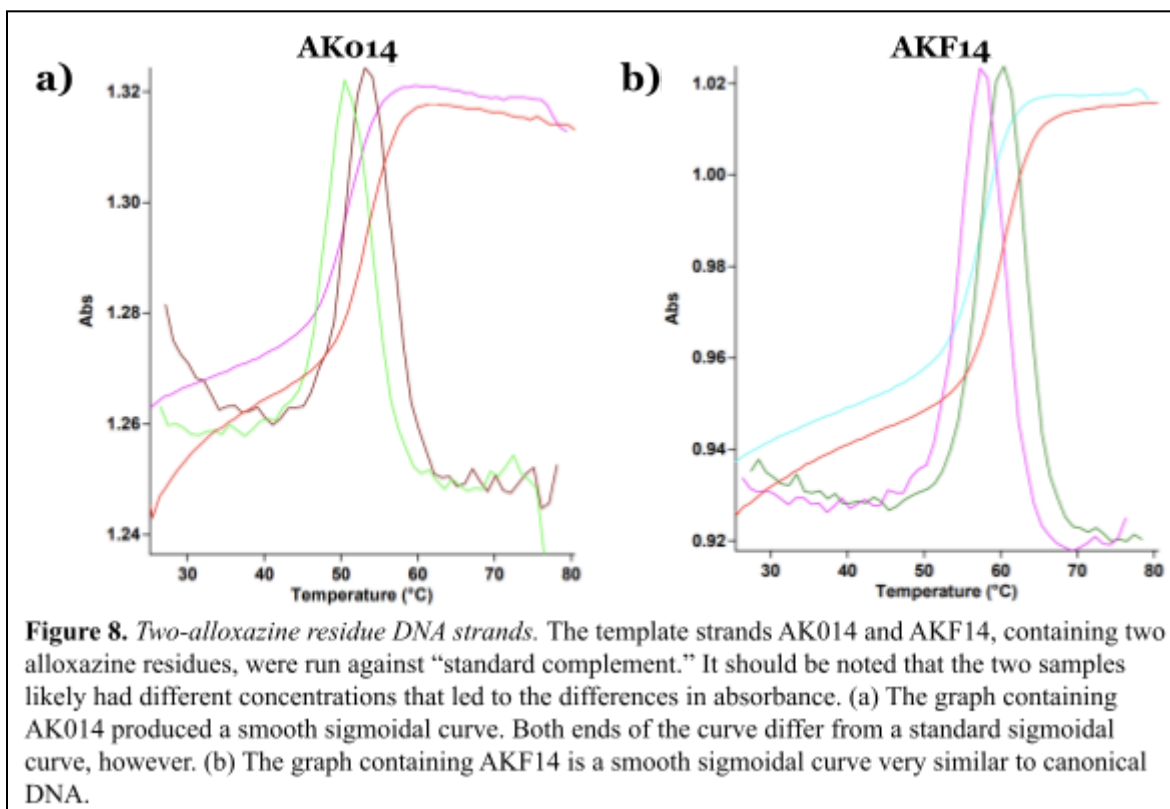
Primer Strand	T _m Value: DNA1-A	T _m Value: AK06	(DNA1-A) - (AK06)
Standard Complement	56.2°C	56.2°C	0°C
Mismatch C	50.2°C	54.1°C	-3.9°C
Mismatch G	52.1°C	56.0°C	-3.9°C
Mismatch T	51.5°C	55.3°C	-3.8°C

Table 2. *DNA1-A and AK06 T_m Comparisons.*

A comparison of the T_m values for each of the primer strands paired with DNA1-A containing no alloxazine, and AK06 containing one alloxazine residue is in Table 2. The T_m values for the three mismatched primer strands was higher when paired with AK06. This could be due to a variety of things, most notably the interactions of the DNA bases with the solvent. The solvent is mostly made up of water. While the residues themselves are not charged, DNA as a whole has a negative charge caused by the phosphate groups in the backbone. Therefore, the water molecules interact with the DNA in solution to neutralize the charges. To replace the water molecules with residues on the other DNA strand, the system requires a large amount of energy. It is possible that the water molecules in solution interact with the residues in the AK06 strand more strongly than DNA1-A residues interact with the solvent, increasing the amount of energy needed to displace the solvent molecules. This general trend of T_m values being higher in samples containing one alloxazine residue compared to canonical DNA was consistent for AKF06, AKF17, and AKF18, and can be found in the supplementary information.

Within the samples containing two alloxazine residues, a sigmoidal curve more similar to DNA1-A/X than AK06/X was produced. As shown in Figure 8(a-b), a smaller hysteresis effect was present in the samples containing two alloxazine residues. The curve for the samples also tended to have more “wobble” near the transition point between heat up and cool down, as seen in both the measurement lines, as well as the first derivative graphs. Both DNA1-A and AK06

paired with the standard complement processed an average T_m value of 56.2°C . The average T_m value for AK014 is 4.4°C lower at 51.8°C . The average T_m value for AKF14, on the other hand, is 2.7°C higher than for DNA1-A and AK06 at 58.9°C . We are unsure why these two samples produced such different average T_m values, but these findings were consistent over multiple experiments.



All samples containing zero, one, or two alloxazine residues produced sigmoidal curves and average T_m values in the mid- to high- 50°C range. For all the samples, the heat up T_m value was higher than the cool down T_m value, indicating a difference in base interactions between heating and cooling the DNA samples. We compared how big of a hysteresis effect alloxazine residues had on the samples by subtracting the cool down T_m value from the heat up T_m value for samples containing zero, one, or two alloxazine residues. The average differences are shown in Figure 12. In general, DNA strands that have either zero or one alloxazine residue have a higher

difference in T_m values than DNA strands that have two alloxazine residues. It is likely that the number of alloxazine residues in each strand of DNA changes the bonding of single strands of DNA, which changes the T_m values for the heat up and cool down cycles.

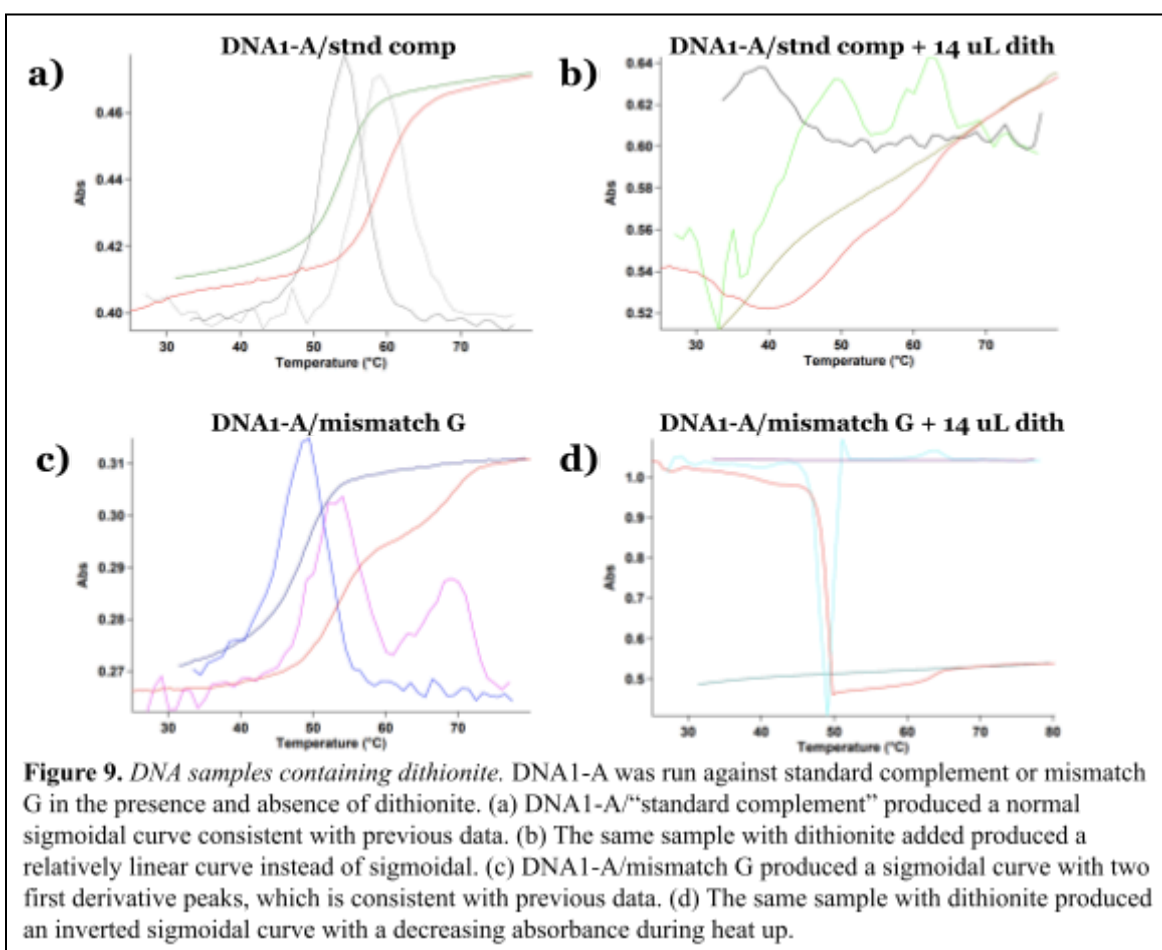
Comparing DNA strands containing solely canonical residues and strands containing one or two alloxazine residues illustrates atypical and non-uniform trends. The average T_m values remain similar when comparing canonical and single-alloxazine DNA strands, but increase or decrease by a few degrees when a second alloxazine residue is added. A similar trend is seen with the hysteresis effect as well. Canonical DNA and single-alloxazine DNA each display a similar hysteresis effect, but the difference in T_m values between cycles decreases when a second alloxazine residue is added to the DNA strand. The base pairing differences between canonical and alloxazine-containing DNA can be measured in a variety of ways and gives insight to the variations in double-stranded DNA helices in the presence of non-canonical residues.

Dithionite reduces DNA samples

Once we established that double-stranded DNA forms with two canonical DNA single strands, as well as single strands of DNA containing alloxazine, we changed the oxidation state of the samples. In previous experiments, the alloxazine residues were oxidized by their environment, which allowed them to bind to adenine residues on the opposite DNA strand. To cause the alloxazine residues to bind P residues, we needed to create a reducing environment..

We began by creating a reducing environment with canonical DNA samples. With the addition of dithionite, both the alloxazine residues and the oxygen in solution were reduced. We began by adding 14 μL 0.1M dithionite. For these early experiments, flavin was used as the indicator for determining if samples were reduced. As a result, after the addition of dithionite, the samples needed to be mixed carefully to diffuse the dithionite and flavin through the entirety of

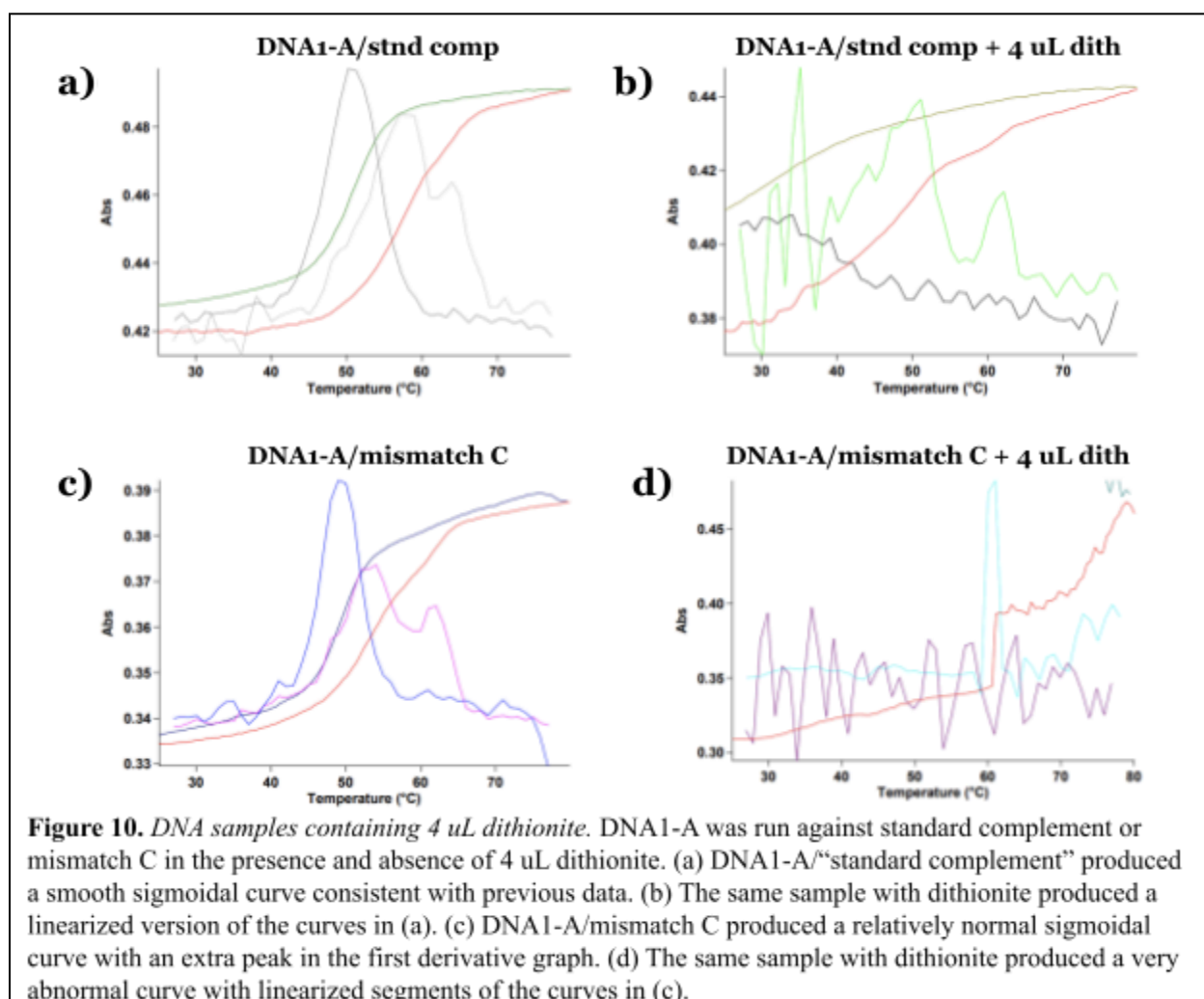
the sample. This process generally invited the sample to be mildly reoxidized, though the reoxidation was likely minimal with such a high concentration of dithionite. The graphs for DNA1-A paired with “standard complement” and “mismatch G” with and without 14 uL 0.1M dithionite are shown in Figure 9.



As evident in Figure 9, the presence of dithionite in the samples produces curves that significantly vary from the expected sigmoidal curve. The heat up and cool down curves become linear or even sigmoidal in the opposite direction for the case of DNA1-A/mismatch G with dithionite (Figure 9d). To determine if dithionite interferes with DNA and at what concentration the interference is relevant, we next tested the samples using 6 uL 0.1M dithionite. The graphs for the samples containing dithionite appeared relatively linear instead of sigmoidal when paired

with both standard complement and mismatch G, indicating that the dithionite is likely the main spectra observed. The T_m values serve as another indication of interference. For DNA1-A paired with the standard complement and 6 uL dithionite, the T_m values were 34.1°C and 38.2°C. For DNA1-A paired with mismatch G and 6 uL dithionite, the T_m values were 63.1°C and 28.9°C.

The very low T_m values, and very large hysteresis effect, in the presence of dithionite convinced us to further lower the concentration of dithionite in the samples. At this point in the experiments, we tested sample reduction by looking for an absorbance peak at 315 nm instead of using flavin as a visual, which decreased the potential for reoxidation. In the presence of 4 uL 0.1M dithionite, the T_m values of the samples looked similar to the samples in the presence of 6 uL dithionite. As shown in Figure 10, the sigmoidal curve of the DNA samples is lost when

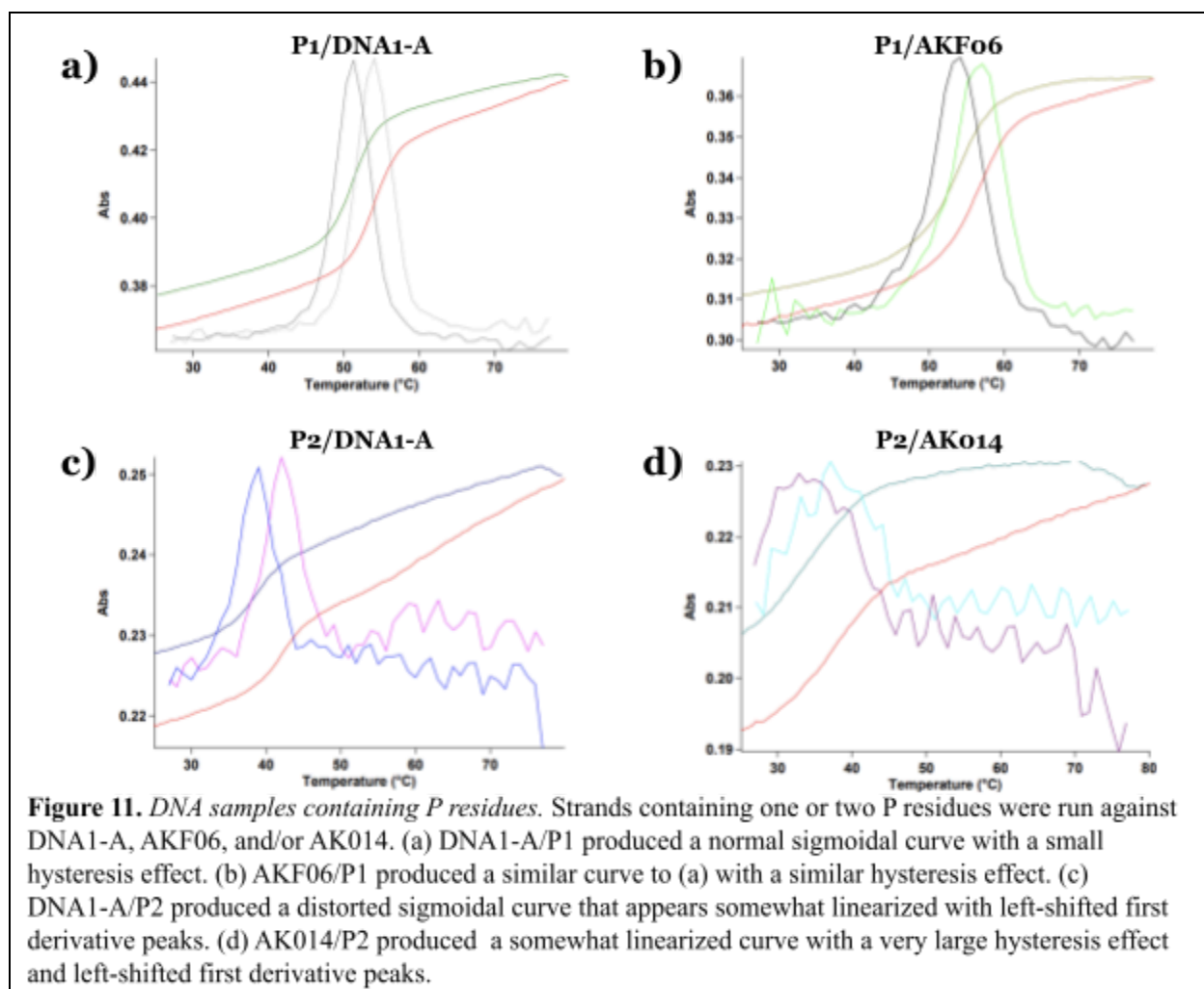


dithionite is present. The curve for DNA1-A/standard complement with 4 uL dithionite (Figure 10b), is significantly closer to the expected sigmoidal curve compared to when 14 uL dithionite is present (Figure 9b). It appears that for both the standard complement and mismatch C with DNA1-A, dithionite is interfering with the DNA interactions or taking priority in the absorbance spectra. The absorbance values at 315 nm for DNA1-A/standard complement with and without 4 uL 0.1M dithionite had a difference of 0.009, and we determined that adding less than 4 uL dithionite would not adequately reduce the samples.

While dithionite is a very powerful reducing agent, the compound interacts with DNA spectra significantly, even at low concentrations. It is likely that if dithionite interferes with DNA interactions, the agent inhibits interactions between strands once they are separated, as indicated by the significantly lower T_m value during the cool down cycle. Therefore, we cannot conclude any significant changes in the structure of double-stranded DNA when the samples are reduced since our reducing agent likely interfered with the data we collected.

Visualizing DNA containing residue P

After unsuccessful experiments with dithionite, we tested DNA strands containing P by pairing them with canonical DNA strands and DNA strands containing alloxazine. The results for the P strands are shown in Figure 11. In general, the sigmoidal curve that was expected is present, though the presence of two P residues distorts the curve in relation to only one P residue.



Analyzing the first derivative graphs of all four samples in Figure 11, we can generally see distinct peaks signifying a specific T_m value. For DNA1-A/P1, AK06/P1, and DNA1-A/P2, it is possible to make out distinct first derivative peaks for the heat up and cool down cycles. For AK014/P2, however, the first derivative peaks are far more rounded and widened, and the graph relating to the sample has largely lost its shape.

We then looked further into why the sigmoidal curve changes so drastically when two *P* residues exist in a DNA strand, but less so when only one *P* residue is present. According to Laos et al⁸, the *P* residue places electron density into the minor groove of DNA. The literature also mentioned that in PCR reactions, pairings containing *P* residues were replaced with C:G pairings

over time due to their similarity in size and hydrogen bonding complementarity. Our research paired the P residue opposite adenine, which varies in size and number of possible hydrogen bonds in comparison to cytosine. Therefore, it may be possible that the P residue and adenine do not form as many, or as stable, hydrogen bonds as thymine paired with adenine. The mismatch base pairing in the middle of the DNA sequences containing P residues may interfere with the resulting shape that the double-stranded DNA takes on. This can be seen in both the shape of the sigmoidal curve for samples containing two P residues, as well as the low T_m values reported for both samples containing two P residues from Figure 11 (Table 3).

DNA strands containing one P residue do not appear to be significantly impacted by the presence of the P residue. It is possible that having only one P residue in the 24-residue DNA sequence does not largely impact the shape of the double-stranded DNA structure, but once two P residues are present in the strand, hydrogen bonding is severely impacted. It appears that introducing a residue that changes the hydrogen bonding complementarity and size of the original residue does impact the shape double-stranded DNA takes on, and the change is further illuminated by increasing the number of non-canonical residues.

Discussion

This research project aimed to understand how non-canonical residues in DNA strands change the way single strands of DNA interact to form double-stranded double helix DNA. By measuring the melting temperature of DNA containing only canonical DNA, and DNA containing two non-standard bases, alloxazine (X) and the P residue, we made inferences about the bonding capabilities and strengths of different strand pairings of DNA. Extensive research in

the binding characteristics of DNA in oxidizing versus reducing environments has not been done, and our research adds to this field. Previous research on oxidized versus reduced DNA samples has shown that 24 nucleotide sequences of DNA containing one or two alloxazine residues exhibit similar spectra and melting temperature curves to purely canonical DNA²⁷. Our research supported this claim that DNA samples containing one or two alloxazine residues likely form similar interactions to canonical DNA. This research project also looked further, past the loss of hydrogen bonding between reduced alloxazine and adenine, and into the hydrogen bond formation between reduced alloxazine and another non-canonical residue, P.

DNA samples containing alloxazine

We began by looking at the spectra and melting curves of canonical DNA. Biological DNA almost always takes on the B-form conformation, therefore the T_m values and spectra for our canonical DNA samples served as a control with which to compare our other samples. We began by testing DNA samples containing a single alloxazine residue in the 24-residue sequence and pairing that strand with a canonical DNA strand. The resulting temperature versus absorbance graphs for the samples looked similar to DNA samples containing only canonical DNA. Both kinds of samples produced sigmoidal curves with similar first derivative peaks (Figure 7). The T_m values for fully canonical DNA and DNA containing one alloxazine residue are identical for pairings with the standard complement, and about 4°C different for the three mismatch primer strands. Generally, the heat up T_m value for canonical DNA was lower than for single-alloxazine DNA, and the cool down T_m value for single-alloxazine DNA samples nearly matched the heat up T_m values for canonical DNA samples. As a result, the temperature versus absorbance graphs for single-alloxazine DNA tended to be more right-shifted than the canonical samples. Previous experimentation has shown that one A:T bond in a DNA sample increases the

T_m value for the sample by 2°C^{28} , which is about half the difference in T_m values between our two samples. When alloxazine is added in the DNA strand, one A:T bond is replaced by an X:A bond. Instead of seeing a T_m difference between the samples of 2°C , our research showed a 4°C difference in T_m values. Additionally, we would expect single-alloxazine DNA to have a lower average T_m value since we displaced an A:T bond, but the opposite is observed (Table 2).

Further experimentation is necessary, but it is likely that alloxazine interacts more strongly with the solution the sample was run in, and more energy is required to break the bonds between strands when one alloxazine residue is present in samples. The structure of single-alloxazine DNA, however, is similar to canonical DNA. One alloxazine present in the 24-nucleotide DNA samples does not seem to largely affect base stacking interactions, and instead likely interferes with base-solvent interactions.

We next tested DNA samples containing two alloxazine residues. The temperature versus absorbance graphs for the double-alloxazine DNA strands produced similar sigmoidal curves, though the ends of the curve were less linear than canonical DNA (Figure 8). Comparing the T_m values for canonical, single-alloxazine, and double-alloxazine DNA paired with the standard complement primer strand, the double-alloxazine DNA samples always varied from the average T_m values of canonical DNA by at least 2°C , but were higher or lower depending on the template strand. We ran multiple experiments with both double-alloxazine samples, and produced similar results each time. We speculate that the difference in T_m values between the samples could be due to alloxazine placement and how those residues interact with the solution and other base pairs in the sample. The hysteresis effect of double-alloxazine DNA compared to canonical and single-alloxazine DNA is also lower. This indicates that double-alloxazine samples have base-base interactions that dominate over the base-solvent interactions that occur after the

strands are separated. Due to the similar heat up and cool down T_m values, it is possible the residues in double-alloxazine DNA interact with the solution on a smaller scale than canonical DNA strands do. Experiments with these three sample types indicate that alloxazine does not change the sigmoidal curve of canonical double-stranded DNA, but the non-canonical residues change the way the residues interact with the solution and with each other, leading to variations in temperature versus absorbance curves.

DNA samples reduced by dithionite

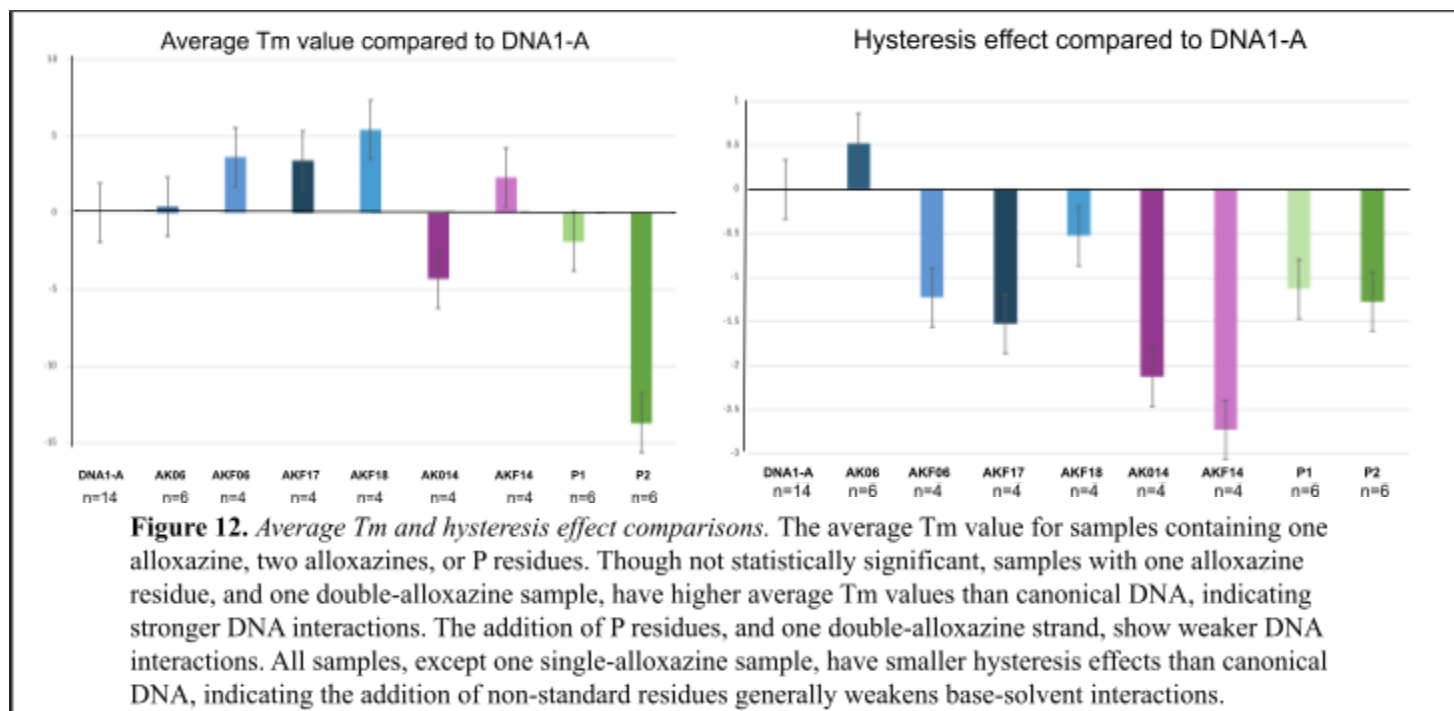
After indicating the way alloxazine manipulates DNA interactions, we reduced the samples to change the base-pairing partner of alloxazine in samples. We tested a range of dithionite concentrations, but the addition of dithionite to our DNA samples ultimately caused interference with our DNA spectra. Canonical DNA containing a large dithionite concentration (14 μ L 0.1M) caused a linearization, or even inversion, of the expected sigmoidal curve (Figure 9). Even in the presence of a lower dithionite concentration (4 μ L 0.1M), the temperature versus absorbance curves were linear and contained sharp jumps in absorbance (Figure 10).

Additionally, when dithionite was added to samples and run days later, the samples containing dithionite produced expected sigmoidal curves. Based on this data, dithionite decomposes into sodium bisulfite and sodium thiosulfate completely within a day and a half. Therefore, the samples that previously contained dithionite likely no longer contained dithionite once they were run through the spectrometer. These results also indicated that the byproducts of dithionite decomposition do not interfere with DNA. When the samples contain fresh dithionite, however, the sigmoidal curve almost completely disappears. We concluded that dithionite does likely interfere with the DNA spectra, especially after the samples have been separated and exist as single DNA strands.

Residue P in DNA samples

The purpose of testing the reducing capabilities of dithionite was to reduce alloxazine residues in samples and base pair the residues to a non-canonical P strand. Despite obtaining poor results using dithionite, we tested strands containing one or two P residues against canonical DNA and single- or double-alloxazine DNA strands in an oxidizing environment. 1P (strands containing one P residue) primer strands paired with both canonical DNA and single-alloxazine DNA produced normal sigmoidal curves (Figure 11). The average T_m values for both samples were lower than when the template strands were paired with the standard complement primer strand, but the curves had a strong first derivative graph and a hysteresis value around 3°C. This data suggests that a single P residue hardly interferes with the Watson-Crick base pairing properties of DNA, though it does interfere a small amount as seen by the lowered average T_m value. Double-stranded DNA containing one P residue displays similar curves to canonical DNA, with slightly weaker interactions between strands. When the samples contained two P residues, however, the base pairing properties of the DNA samples appeared to be changed. As shown in Figure 11(c-d), samples containing two P residues produced a distorted sigmoidal curve with a large hysteresis effect. The average T_m values were 16°C (P2/DNA1-A) to 26°C (P2/AK014) lower than DNA1-A paired with the standard complement. The significant decrease in average T_m values indicates that the base pairing between strands is much weaker than in canonical DNA. The single strands of DNA interact strongly with the solution and those interactions are hard to break to replace the base-solvent interactions with base-base interactions. Double-stranded DNA containing two P residues appears to still produce a B-form conformation according to data from Ayman, though with altered base stacking. The base stacking capabilities of the residues, however, seems to weaken as more P residues are added to the sequences. Base

stacking is minorly interfered in the presence of one P residue, and more significantly interfered when two P residues are present.



Future directions

Current literature heavily focuses on the ability of alloxazine to selectively bind to adenine over thymine, guanine, and cytosine^{27, 29}, which aligns with our research focusing on alloxazine replacing thymine in a DNA sample. Our research largely agreed with the current literature in that DNA strands containing one or two alloxazine residues produce DNA double-helices with minimal base stacking disruptions. Differing from our research, however, current literature examined the base pairing properties of alloxazine in a reducing environment. A large limitation of our research revolves around the interactions between dithionite and DNA, as we were largely unable to produce significant data for reduced DNA samples. Previous research has also been conducted to determine the base pairing capabilities of the P residue⁸.

Like our research, literature focuses on the potential of the P residue to pair with other non-canonical bases. While our research focused on P paired with alloxazine specifically, the data collected during our experiments aligns with current research in that the P residue has the capacity to make hydrogen bonds using its two acceptor and one donor group. To date, no research has put these two niches together to study the capability of P to bind reduced alloxazine, however.

Biological technologies have improved significantly over the past decade, including in the field of DNA nanorobots³⁰. The potential to control cellular behavior to a variety of stimuli allows for new possibilities in medicinal fields. An important segment of DNA nanotechnology is the ability to manipulate the base pairing and base stacking characteristics of DNA, including non-canonical DNA. Our research focused on the ability of two non-canonical residues to interact and form base pairs that influence the resulting shape of double-stranded double-helix DNA. Future research needs to focus on finding an appropriate reducing agent for samples containing alloxazine. Once an appropriate agent is determined, strands containing one or two alloxazine residues can be paired with strands containing one or two P residues to determine if the B-form of double-stranded DNA is altered. It is also important to gain further understanding of the actual interactions the two strands have with each other. X-ray crystallography or a different imaging technique, can be used to look at the physical structures of each non-canonical base pair, as well as the interactions between the residues in a short sequence of DNA. Our research aimed to understand how the double-stranded double helix changed in the presence of non-canonical residues, and how these changes can be manipulated to enhance DNA nanotechnology and origami in the future of gene therapy and personalized medicine.

Materials and Methods

Annealing DNA samples

To create samples of DNA that were double stranded, it was necessary to anneal two single-stranded DNA components. The DNA strands contained either only standard base pairs, standard base pairs and alloxazine (represented as X), or standard base pairs and residue P. The sequences containing standard base pairs and standard base pairs plus alloxazine were purchased from Integrated DNA Technologies (IDT). The sequences containing residue P were purchased from Firebird Biomolecular Sciences. The two strands in each sample complimented each other in the 5' → 3' direction, with examples of pairings being:

<u>Primer</u>	<u>Template</u>
Standard compliment	DNA1-A
5'-AAA GGA GAA GAA GGA GAA GAG GAA-3'	5'-TTC CTC TTC TCC TTC TTC TCC TTT-3'
Standard compliment	AK08
5'-AAA GGA GAA GAA GGA GAA GAG GAA-3'	5'-TTC CTC TTC TCC XX C TTC TCC TTT-3'
2P	DNA1-A
5'-AAG PG AAG AGG AAG AAG P GG AAA-3'	5'-TTC CTC TTC TCC TTC TTC TCC TTT-3'

A full list of the sequences containing alloxazine is found in Supplementary Figure 1.

Samples were made up to be 1 mL and contained DNA, salt, water, and buffer. 100 uL 1M NaCl was added to stabilize the DNA sequences by decreasing electrostatic repulsions within the negatively-charged phosphate backbone²². For multiple experiments, an additional 5 mL 5 mM MgCl₂ was added to further stabilize the DNA within the samples. 10 uL 1M HEPES (2-[4-(2-hydroxyethyl)piperazin-1-yl]ethanesulfonic acid; Research Products International Corporation) served as a buffer to keep the samples at a consistent biochemically relevant pH

while the separation and annealing of DNA occurred. The amount of DNA added to each sample depended on the concentration of the stock solution for each strand. The concentration of each stock was determined using its absorbance value at 260 nm. After the salt, buffer, and DNA were included in each sample, deionized water was added to fill the remaining volume until 1 mL of sample was reached.

Once the samples were made up in 1.7 mL tubes (OPTIMUM BESTUBES), they were added to a water bath that was kept at 70°C. The tubes were incubated at 70°C for two minutes, then left in the water as the bath was turned off. The water was given time to cool off to 25°C over a two hour period. This slow cooling process allowed the DNA to correctly anneal to its base pair and form a correct double helix structure. Once the DNA samples were annealed, they were either used immediately for experimentation or were placed in the freezer to be used at another date.

Preparing reduced samples

After the tubes of DNA samples were annealed in a water bath and cooled to room temperature, the DNA was present in an oxidized state. For some experiments, it was important that the DNA in the samples be reduced in order to study the way the double-helix structure of DNA changes when the strands include reduced base pairs. Dithionite was added to samples as a reducing agent for both the base pairs in DNA, as well as the oxygen in solution.

1M sodium dithionite (sodium hydrosulfite; Sigma-Aldrich) was utilized by adding the powdered form of sodium hydrosulfite to deionized water. It was important to make up the 1M dithionite in a container that contained as little oxygen as possible, so that the dithionite would be minimally oxidized before adding the solution to samples²³. It was also important to make up the 1M dithionite fresh every day of an experiment requiring the compound. Dithionite

decomposes in aqueous solutions to create the byproducts sodium thiosulfate and sodium bisulfite²⁴. Some papers show that in near-neutral buffered solutions, dithionite could be present for up to 50 days²⁵. Our personal research, however, indicated that dithionite is untraceable in a sample after just two days of being added.

Samples were made up in 1.7 mL tubes (OPTIMUM BESTUBES). Between 4 uL and 6 uL of 1M dithionite were added at the same depth in each sample, and the samples were carefully mixed to introduce as little oxygen as possible. The samples were then transferred from tubes to rectangular 10.0 mm path length cuvettes (Fisherbrand Semi-Micro Quartz Cuvettes). 2 mL of sample was added to each cuvette, which was enough to just overfill the cuvette. The cap was then carefully placed on the cuvette to avoid producing air bubbles. The cuvette was wiped with a Kimwipe to ensure the the sides of the cuvette were free of any impurities before being run through the spectrometer.

Initially, the presence and strength of dithionite was measured using riboflavin. Riboflavin is bright yellow in color when the compound is oxidized, and colorless when reduced. Therefore, riboflavin was added to the samples containing DNA to give the solutions a faint yellow color. Once the dithionite was added to the samples, we could establish whether the sample was reduced by visually determining if the sample lost its yellow hue. We also discovered, however, that when in solution, dithionite has a strong absorbance around 315 nm when run through the spectrometer (Beckman DU640). The samples were prepared in the ways mentioned above and the absorbance of the sample from 250 nm to 500 nm was taken. If there was a small peak in the graph around 315 nm, then we could determine that the concentration of dithionite was correct and the sample was properly reduced. Because the absorbance graph of the samples could be taken easily and were more consistent and accurate than visual observation, we

primarily used the latter method of spectroscopy to determine reduction and stopped adding riboflavin to the samples shortly after discovering the method.

Visualizing T_m values using spectroscopy

The melting temperature (T_m) of DNA is defined as the temperature at which half of the DNA in a sample is duplexed and the other half is free in the solution²⁶. T_m is a good indicator of the thermal stability and base interactions in DNA, and was the primary measurement in our research.

We measured the T_m value of our samples using a UV-Vis spectrometer (Varian Cary 100 Bio). 1 mL of each sample was transferred into rectangular 10.0 mm path length cuvettes (Fisherbrand Semi-Micro Quartz Cuvettes). To reduce the loss of sample through evaporation during heat up, each cuvette was capped. The samples were placed inside the instrument and the resulting temperature versus absorbance curves could be seen on the attached computer monitor. The spectrometer took multiple measurements at each degree from 25°C to 80°C, and ramped up 1 degree every minute. After the machine ran through its ramp up and ramp down heat cycle, we took the first derivative of each graph to find the exact T_m value for the two curves. Generally, the cool down curve had a lower T_m value for the sample when compared to the heat up curve. The samples could then be transferred back into 1.7 mL tubes (OPTIMUM BESTUBES) to be frozen.

We also used circular dichroism spectroscopy (Applied Photophysics) as a more generalized method for obtaining broad T_m trends for the DNA samples. We prepared 170 mL of 0.2 mg/ml samples and transferred the contents into 1 mm path length flat cuvettes (Applied Photophysics). We then ran the spectra of the samples from 210 nm to 340 nm at a range of temperatures between 20°C and 80°C. While these experiments did not provide exact T_m values

for the DNA samples, they did allow us to see general trends in the spectra of our DNA samples as temperature increased steadily.

Both UV-Vis spectroscopy and CD spectroscopy provided insight on the behavior of DNA as environment, temperature, and redox state shifted. The characteristic peak of DNA at 260 nm was a constant that ensured our data was valid and related to the structure of DNA.

Determining concentration of stocks

To run our DNA samples through the UV-Visible spectrometer and the CD spectrometer, we had to ensure that the concentration of DNA was appropriate within the sample. Incorrect concentrations cause the absorbance of light at 260 nm within the samples to be too low to properly perceive, or too high for the machine to accurately read. The strands of DNA we used for the experiments (Integrated DNA Technologies) were 1 mM stocks that were diluted into the concentration we needed for each experiment.

To verify the concentration of the stocks, we created a 1:500 dilution of each DNA strand stock and obtained their respective spectras. We then pinpointed the absorbance of the DNA strand at 260 nm. We could then use the Beer-Lambert law (Equation 1) to determine the concentration of the stock sample. A is the absorbance of the sample at 260 nm. ϵ is the extinction coefficient of the sample and is measured in $\text{L mol}^{-1} \text{cm}^{-1}$. The extinction coefficient depends on the bases that are present in the DNA strand and can easily be determined on the IDT website. l is the path length of the cuvette and is measured in cm. By solving for C , the concentration of the DNA sample is calculated in mol/L (molarity).

$$A = \epsilon l C$$

Equation 1. The Beer-Lambert Law

Once the concentration of the stocks was verified, we could determine how much of the stock solution needed to be added to each sample to create a 1 μM sample of DNA. The samples were made up to be 1 mL, with 0.1 M NaCl, 0.01 M HEPES, 1 μM of the primer strand, and 1 μM of the template strand. Deionized water was added as the remaining compound until the sample reached 1 mL. These samples were used for the UV-Visible spectrometer.

The CD spectrometer required that samples be 0.1 mg/ml and 170 μL . The same process listed above was used to create these samples as well, though with a much smaller sample volume and concentration.

The absorbance of samples provided an accurate measurement of the concentration of our samples. Absorbance was used to ensure that our samples were within an appropriate concentration range for both types of spectrometers, and that our data was accurate and useful as a result.

Analysis of T_m values

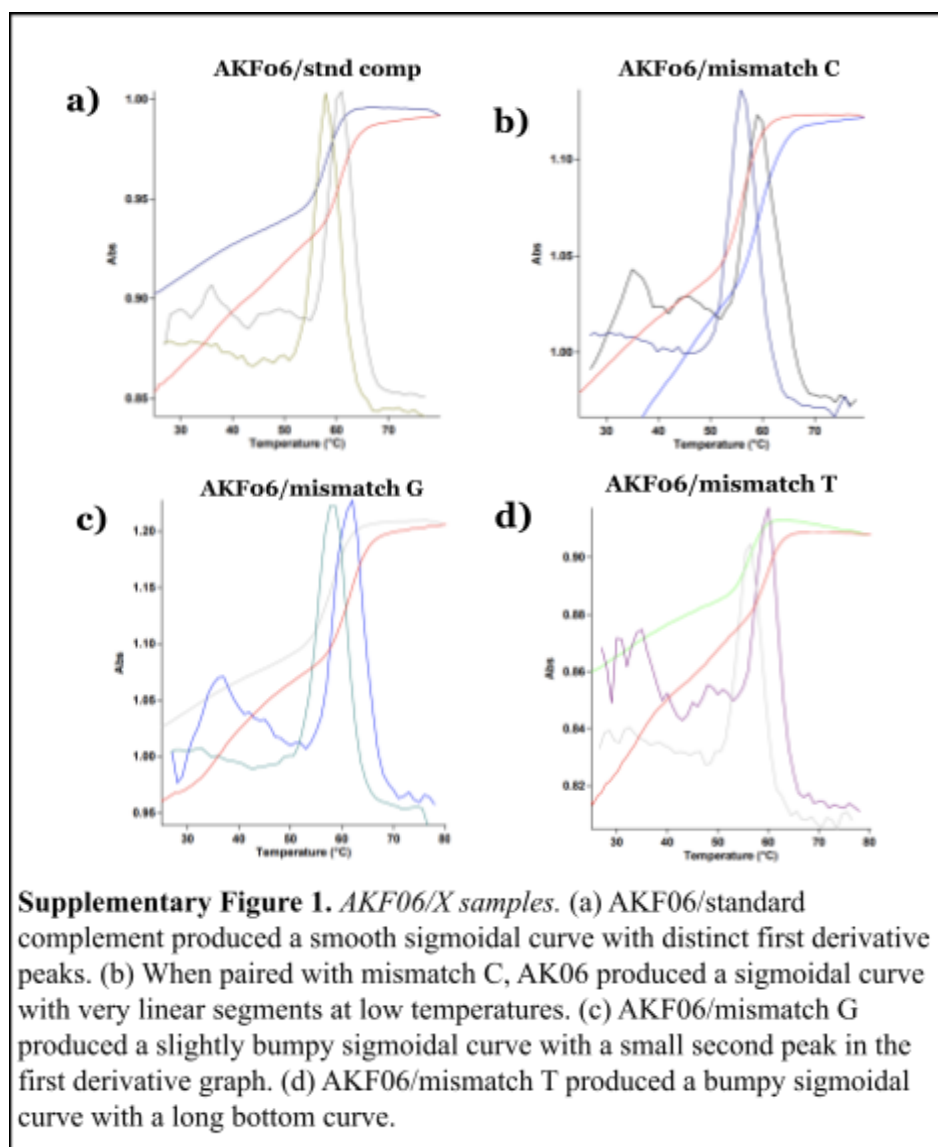
To compare the melting temperature of each DNA combination, we created a table in an excel spreadsheet. Along the side of the table, we listed the primer strands, and along the top of the table, we listed the template strands, as shown in Table 3.

The excel sheet contains the average T_m value for every combination of DNA strands tested. After each experiment, the new T_m value was added to the cell and was considered into the average. Each set of DNA has at least two experimental T_m values that are used for the average calculation, but some cells have up to 17 T_m values. From the excel spreadsheet, we were able to compare any number of T_m values through graphs and simple algebraic equations. The table allowed us to quickly visualize the average T_m value for a set of DNA and determine which experiments we wanted to proceed with.

	comp	comp + 4uL dith	AKF06 (1X)	AK014 (2X)	AKF18 (1X)	AKF17 (1X)	AK06 (1X)	AKF14 (2X)	AKF08 (2X)	AK08 (2X)	AK010 (4X)
“A”	55.49	36.82	59.70	51.75	61.45	59.45	56.43	58.35	55.80	54.55	44.90
“C”	52.44	42.76	55.40	■	54.10	■	54.35	■	■	■	■
“G”	50.76	■	55.10	■	57.35	■	56.30	■	■	■	■
“T”	51.45	■	54.15	■	56.50	■	55.45	■	■	■	■
P1	54.15	■	55.85	■	■	■	■	■	■	■	■
P2	42.33	■	■	37.25	■	■	■	■	■	■	■

Table 3. *T_m* values for primer and template strands.

Supplementary Information



AK01	T	T	A	T	T	A	T	T	A	T	T	A	T	T	A	T	T	A	T	T	A	
AK02	T	T	A	T	T	A	T	T	A	T	T	A	X	T	A	T	T	A	T	T	A	
AK04	T	T	A	T	T	A	T	T	A	T	T	A	X	T	A	T	T	A	T	T	A	
AK05	T	T	C	T	T	C	T	T	C	T	T	C	X	T	C	T	T	C	T	T	C	
AK06	T	T	C	C	T	C	T	T	C	T	C	C	X	T	C	T	T	C	T	C	C	250 μ M
AK07	T	T	C	C	T	C	T	T	C	T	C	C	T	T	C	T	T	C	T	C	C	
AK08	T	T	C	C	T	C	T	T	C	T	C	C	X	X	C	T	T	C	T	C	C	3580 μ M
AK09	T	X	C	C	T	C	X	T	C	X	C	C	X	T	C	X	T	C	X	C	C	360 μ M
AK010	T	X	C	C	T	C	T	T	C	X	C	C	T	T	C	X	T	C	T	C	C	8700 μ M
AK014	T	T	C	C	X	C	T	T	C	T	C	C	T	T	C	T	T	C	X	C	C	6380 μ M
AKF06	T	T	C	C	T	C	T	T	C	T	C	C	X	T	C	T	T	C	T	C	C	1660 μ M
AKF07	T	T	C	C	T	C	T	T	C	T	C	C	T	T	C	T	T	C	T	C	C	
AKF08	T	T	C	C	T	C	T	T	C	T	C	C	X	X	C	T	T	C	T	C	C	1560 μ M
AKF09	T	X	C	C	T	C	X	T	C	X	C	C	X	T	C	X	T	C	X	C	C	
AKF10	T	X	C	C	T	C	T	T	C	X	C	C	T	T	C	X	T	C	T	C	C	
AKF14	T	T	C	C	X	C	T	T	C	T	C	C	T	T	C	T	T	C	X	C	C	2390 μ M
AKF17	X	T	C	C	T	C	T	T	C	T	C	C	T	T	C	T	T	C	T	C	C	3330 μ M
AKF18	T	T	C	C	T	C	T	T	C	T	C	C	T	T	C	T	T	C	T	C	C	2460 μ M

Supplementary Table 1. *DNA sequences containing alloxazine.*

Acknowledgements

I would like to thank Dr. Robert Kuchta for allowing me to pursue research in his lab and for his support over the many summers and semesters. I would also like to thank Ana Mirita for her suggestions, listening ear, and friendship as the research for this thesis was completed. I would like to give a big thank you to Stephanie Renfrow for her feedback and support on the many drafts of this paper. Additionally, I would like to thank Dr. Annette Erbse and the Shared Instrument Pool (SIP). The training I received on the circular dichroism machine was vital for this research project, and couldn't have been done without these facilities. There have been many

individuals who have made this research possible, and this paper would not have been produced without their encouragement and support.

References

1. National Library of Medicine. “The Discovery of The Double Helix, 1951-1953 | Francis Crick - Profiles in Science.” *U.S. National Library of Medicine*, National Institutes of Health, profiles.nlm.nih.gov/spotlight/sc/feature/doublehelix
2. Rivard, L. “Nucleotides and Bases.” *Genetics Generation*. 16 Aug 2023. knowgenetics.org/nucleotides-and-bases/
3. Pray, L. “Discovery of DNA structure and function: Watson and Crick.” *Nature Education*. 2008;1(1):100. <https://www.nature.com/scitable/topicpage/discovery-of-dna-structure-and-function-watson-397/>
4. Hardison, R. “2.5: B-Form, A-Form, and Z-Form of DNA.” *Biology LibreTexts*. 19 July 2021. [bio.libretexts.org/Bookshelves/Genetics/Working_with_Molecular_Genetics_\(Hardison\)/Unit_1%3A_Genes_Nucleic_Acids_Genomes_and_Chromosomes/2%3A_Structures_of_Nucleic_Acids/2.5%3A_B-Form_A-Form_and_Z-Form_of_DNA](https://bio.libretexts.org/Bookshelves/Genetics/Working_with_Molecular_Genetics_(Hardison)/Unit_1%3A_Genes_Nucleic_Acids_Genomes_and_Chromosomes/2%3A_Structures_of_Nucleic_Acids/2.5%3A_B-Form_A-Form_and_Z-Form_of_DNA).
5. Terekhova IV, Tikhova MN, Volkova TV, et al. “Inclusion complex formation of α - and β -cyclodextrins with riboflavin and alloxazine in aqueous solution: thermodynamic study.” *J Incl Phenom Macrocycl Chem*. 2011:69, 167–172. doi:10.1007/s10847-010-9827-z
6. Hustad S, McKinley MC, McNulty H, Schneede J, Strain JJ, Scott JM, Ueland PM. “Riboflavin, Flavin Mononucleotide, and Flavin Adenine Dinucleotide in Human Plasma and Erythrocytes at Baseline and after Low-Dose Riboflavin Supplementation.” *Clinical Chemistry*. 1 Sep 2002:48(9), 1571-1577. doi:10.1093
7. Cagardová, D, et al. “Spectroscopic Behavior of Alloxazine-Based Dyes with Extended Aromaticity: Theory vs Experiment.” *Optical Materials*. 28 May 2021. doi: 10.1016
8. Laos R, Lampropoulos C, Benner S. “The surprising pairing of 2-aminoimidazo[1,2-a][1,3,5]triazin-4-one, a component of an expanded DNA alphabet.” *Acta Crystallographica Section C: Structural Chemistry*. Jan 2019:75. doi:10.1107/S2053229618016923
9. Hintz MJ, Peterson JA. “Kinetic Investigation of the Reduction of Cytochrome P-450_{CAM} by Sodium Dithionite.” *Academic Press*. 1980:339-342. doi:10.1016/B978-0-12-187701-9.50065-6

10. Mundy BP, et al. *Name Reactions and Reagents in Organic Synthesis* Bradford P. Mundy, Michael G. Ellerd, Frank G. Favaloro, JR. Interscience, 2005.
11. Vegunta VL. "A study on the thermal stability of sodium dithionite using ATR-FTIR spectroscopy." *KTH Royal Institute of Technology*. Jun 2016.
<https://kth.diva-portal.org/smash/get/diva2:1052027/FULLTEXT01.pdf>
12. Millipore Sigma. "HEPES." <https://www.sigmaaldrich.com/US/en/product/sigma/h3375>
13. Ali V, Shigeta Y, Tokumoto U, et al. "An Intestinal Parasitic Protist, *Entamoeba histolytica*, Possesses a Non-redundant Nitrogen Fixation-like System for Iron-Sulfur Cluster Assembly under Anaerobic Conditions." *The Journal of Biological Chemistry*. May 2004:279(16), 16863-74. doi: 10.1074/jbc.M313314200
14. Hayakawa Y, Banno A, Kitagawa H, et al. "Reduction-Responsive DNA Duplex Containing *O*6-Nitrobenzyl-Guanine." *ACS Omega*. 31 Aug 2018:3(8), 9267–9275. doi: 10.1021/acsomega.8b01177
15. Tom J. "UV-Vis Spectroscopy: Principle, Strengths and Limitations and Applications." *TechnologyNetworks*. 18 Dec 2023.
<https://www.technologynetworks.com/analysis/articles/uv-vis-spectroscopy-principle-strengths-and-limitations-and-applications-349865>
16. University of Tennessee, Knoxville. "The EM Spectrum." <http://labman.phys.utk.edu/phys222core/modules/m6/The%20EM%20spectrum.html>
17. Promega. "Why Does Denatured DNA Absorb More Ultraviolet Light than Double-Stranded DNA?" *Promega Corporation*. 2024.
www.promega.com/resources/pubhub/enotes/why-does-denatured-dna-absorb-more-ultraviolet-light-than/
18. Hurlburt N. "Circular Dichroism." *Biology LibreTexts*.
[https://chem.libretexts.org/Bookshelves/Physical_and_Theoretical_Chemistry_Textbook_Maps/Supplemental_Modules_\(Physical_and_Theoretical_Chemistry\)/Spectroscopy/Electronic_Spectroscopy/Circular_Dichroism](https://chem.libretexts.org/Bookshelves/Physical_and_Theoretical_Chemistry_Textbook_Maps/Supplemental_Modules_(Physical_and_Theoretical_Chemistry)/Spectroscopy/Electronic_Spectroscopy/Circular_Dichroism)
19. Burndt KD. "Circular dichroism spectroscopy." *Birkbeck, University of London*. 31 May 1996.
https://www.cryst.bbk.ac.uk/PPS2/course/section8/ss-960531_21.html
20. Kypr J, Kejnovská I, Renciuk D, Vorlicková M. "Circular dichroism and conformational polymorphism of DNA." *Nucleic Acids Res*. 2009 Apr:37(6), 1713-25. doi: 10.1093/nar/gkp026
21. Que L, Zhang X, Ji J, Gao L, Xie W, Liu L, Ding X. "Numerical simulation and experimental research progress of phase change hysteresis: A review." *Energy and Buildings*. 15 Dec 2021:253. doi: 10.1016/j.enbuild.2021.111402

22. Singh N, Singh A. "Effect of salt concentration on the stability of heterogeneous DNA." *Physica A*. 28 Aug 2014:419, 328-334. doi: 10.1016/j.physa.2014.10.029
23. Tao Z, Goodisman J, Souid AK. "Oxygen Measurement via Phosphorescence: Reaction of Sodium Dithionite with Dissolved Oxygen." *J. Phys. Chem. A*. 12 Sep 2007:112(7), 1511-1518. doi: 10.1021/jp710176z
24. BYJU. "Sodium Thiosulfate (Na₂S₂O₃)." *BYJU's*. 2024.
<https://byjus.com/chemistry/sodium-thiosulfate/>
25. Telfeyan K, Migdisov AA, Pandey S, Vesselinov VV, Reimus PW. "Long-term stability of dithionite alkaline anaerobic aqueous solution." *Applied Geochemistry*. Feb 2019:101, 160-169. doi: 10.1016/j.apgeochem.2018.12.015
26. Millipore Sigma. "Oligonucleotide Melting Temperature." *Millipore Sigma*. 2024.
<https://www.sigmaaldrich.com/US/en/technical-documents/protocol/genomics/pcr/oligos-melting-temp>
27. Alawneh A, Wettasinghe AP, McMullen R, Seifi MO, Breton I, Slinker JD, Kuchta RD. "A Redox-Reversible Switch of DNA Hydrogen Bonding and Structure." *ACS Applied Bio Materials*. 8 July 2024:7(8). doi: 10.1021/acsabm.4c00529
28. Hershell G. "Melting temperature (T_m) value meaning." *ResearchGate*. 5 August 2019.
https://www.researchgate.net/post/Melting_temperature_Tm_value_meaning
29. Rajendar B, Nishizawa S, Teramae N. "Alloxazine as a ligand for selective binding to adenine opposite AP sites in DNA duplexes and analysis of single-nucleotide polymorphisms." *Org Biomol Chem*. 7 January 2008:4. doi:10.1039/B719786A
30. Nummelin S, Shen B, Piskunen P, Liu Q, Kostianen MA, Linko V. "Robotic DNA Nanostructures." *ACS Synth Biol*. 21 Aug 2020; 9(8), 1923–1940. doi: 10.1021/acssynbio.0c00235